Ginkgo biloba extract (GbE) enhances the anti-atherogenic effect of cilostazol by inhibiting ROS generation

In-Hyuk Jung[1,2]*, You-Han Lee[1,3]*, Ji-Young Yoo[1], Se-Jin Jeong[1], Seong Keun Sonn[1], Jong-Gil Park[1,3], Keun Ho Ryu[4], Bong Yong Lee[4], Hye Young Han[4], So Young Lee[4], Dae-Yong Kim[2], Hang Lee[3] and Goo Taeg Oh[1,5]

[1]Division of Life and Pharmaceutical Sciences
Ewha Womans University
Seoul 120-750, Korea
[2]Department of Veterinary Pathology
[3]Department of Veterinary Biochemistry
College of Veterinary Medicine
Seoul National University
Seoul 151-742, Korea
[4]Pharmacology Team
Life Science R&D Center
SK Chemicals
Suwon 440-745, Korea
[5]Corresponding author: Tel, 82-2-3277-4253;
Fax, 82-2-3277-3760; E-mail, gootaeg@ewha.ac.kr
*These authors contributed equally to this work.
http://dx.doi.org/10.3858/emm.2012.44.5.035

Accepted 18 January 2012
Available Online 27 January 2012

Abbreviations: ApoE, apolipoprotein E; cilostazol, 6-[4-(1-cyclohexyl-1*H*-tetrazol-5-yl) butoxy]-3,4-dihydro-2(1*H*)-quinolinone; GbE, *Ginkgo biloba* extract; MCP-1, monocyte chemoattractant protein-1; ROS, reactive oxygen species; VCAM-1, vascular cell adhesion molecule-1

Abstract

In this study, the synergistic effect of 6-[4-(1-cyclohexyl-1*H*-tetrazol-5-yl) butoxy]-3,4-dihydro-2(1*H*)-quinolinone (cilostazol) and *Ginkgo biloba* extract (GbE) was examined in apolipoprotein E (ApoE) null mice. Co-treatment with GbE and cilostazol synergistically decreased reactive oxygen species (ROS) production in ApoE null mice fed a high-fat diet. Co-treatment resulted in a significantly decreased atherosclerotic lesion area compared to untreated ApoE mice. The inflammatory cytokines and adhesion molecules such as monocyte chemoattractant-1 (MCP-1), soluble vascular cell adhesion molecule-1 (sVCAM-1), and VCAM-1 which can initiate atherosclerosis were significantly reduced by the co-treatment of cilostazol with GbE. Further, the infiltration of macrophages into the intima was decreased by co-treatment. These results suggest that co-treatment of GbE with cilostazol has a more potent anti-atherosclerotic effect than treatment with cilostazol alone in hyperlipidemic ApoE null mice and could be a valuable therapeutic strategy for the treatment of atherosclerosis.

Keywords: atherosclerosis; cilostazol; cytokines; disease models, animal; *Ginkgo biloba*; inflammation; macrophages; reactive oxygen species

Introduction

Atherosclerosis is a chronic inflammatory disease of blood vessels characterized by slow thickening of arterial walls due to the build-up of fatty material (Chen *et al*., 2003; Park *et al*., 2008). During the early stages of atherosclerosis, cholesterol accumulation in the intima induces endothelial cells in the arteries to express adhesion and chemoattractant molecules, such as vascular cell adhesion molecule-1 (VCAM-1) and monocyte chemoattractant protein-1 (MCP-1) (Otsuki *et al*., 2001; Lee *et al*., 2005; Yun *et al*., 2009). Reactive oxygen species (ROS), including superoxide, are implicated in the cellular response to a variety of inflammatory stimuli, including atherosclerosis (Zhou *et al*., 2000; Altiok *et al*., 2006; Rhein *et al*., 2010).

6-[4-(1-cyclohexyl-1*H*-tetrazol-5-yl) butoxy]-3,4-dihydro-2(1*H*)-quinolinone(cilostazol) is a selective phosphodiesterase III inhibitor that increases the intracellular cyclic adenosine monophosphate (cAMP) concentration (Kim *et al*., 2002, 2006; Lim *et al*., 2009). Cilostazol inhibits cytokine-induced nuclear factor-κB (NF-κB) activation *via* AMP-activated protein kinase activation in vascular endothelial cells (Nakamura *et al*., 2005; Hattori *et al*., 2009). Besides anti-platelet and anti-vasoconstrictive properties (Wang *et al*., 2003; Mohamed, 2009), cilostazol promotes cholesterol efflux by regulating cholesterol uptake- or efflux-related genes, such as scavenger receptors (e.g., SR-A and CD36) (Shin *et al*., 2004; Gomez and Qureshi, 2009) and ABCA1/ABCG1 (Nakaya *et al*., 2010) in macrophages. Cilostazol inhibits NAD(P)H oxidase-dependent superoxide formation and cytokine release concomitant with the suppression of atherosclerotic plaque formation in LDL receptor-null mice (Yun *et al*., 2009).

Ginkgo biloba extract (GbE), a Chinese herbal medicine extracted from leaves of the *Ginkgo biloba* tree (Chen *et al*., 2003), has increasingly been shown to have a variety of beneficial effects in cerebral and peripheral arterial diseases, especially dementia and claudication (Wei *et al*., 1999; Lee *et al*., 2001; Wang *et al*., 2003; Sethi and Arora, 2008). GbE contains flavone glycoside and 6% terpene lactones (ginkolides, bilobalide), known free radical scavengers (Kampkotter *et al*., 2007; Ou *et al*., 2009). GbE also exerts an anti-phlogistic effect on inflammatory cells by suppressing active oxygen and nitrogen species production (Ou *et al*., 2009). For example, the terpene lactone component in GbE inhibits nitric oxide (NO) production in macrophages infiltrating a Candida albicans-mediated arthritic inflammation site (Lippi *et al*., 2007). Recently, GbE was shown to reduce the formation of atherosclerotic nanoplaques (Rodriguez *et al*., 2007), attenuate oxLDL-induced oxidative functional damage in endothelial cells (Ou *et al*., 2009), and decrease the levels of highly atherogenic lipoprotein (Lippi *et al*., 2007; Rodriguez *et al*., 2007; Siegel *et al*., 2007). Thus, GbE may at least partially have an anti-inflammatory effect, and supplementation with GbE may have clinical value in patients at risk for increased serum concentrations of lipoprotein (Lippi *et al*., 2007).

The combination of cilostazol and probucol, another potent lipid-soluble antioxidant, displayed a synergistic effect on the suppression of ROS and inflammatory markers in human coronary artery endothelial cells (Park *et al*., 2008). Moreover, GbE may potentiate the anti-platelet effect of cilostazol without prolonging bleeding or coagulation times (Ryu *et al*., 2009). Although the anti-atherogenic effects of both cilostazol and GbE have been suggested in previous studies, the synergistic effect of these two compounds on atherosclerosis has not been investigated.

Here, we show that combination therapy consisting of cilostazol and GbE may exert enhanced anti-atherogenic effects compared to treatment with cilostazol alone.

Results

GbE increases the anti-oxidant activity of cilostazol

Both cilostazol and GbE reduce ROS production in a variety of cell types (Wei *et al*., 1999; Kim *et al*., 2002; Kampkotter *et al*., 2007) and have a synergistic effects in treating atherothrombosis without adverse side effects such as the prolongation of bleeding time or coagulation time (Liu *et al*., 2009). Therefore, we postulated that combinative treatment of an atherosclerotic mouse model with GbE and cilostazol would decrease superoxide production in atherosclerotic plaque more than treatment with cilostazol alone. Superoxide production in the plaque lesion of the aortic root was decreased in all the treated groups, and also was lower in the high dose co-treatment group than cilostazol alone (Figure 1). This suggests that co-treatment of cilostazol with GbE synergistically inhibits ROS production in the development of atherosclerosis.

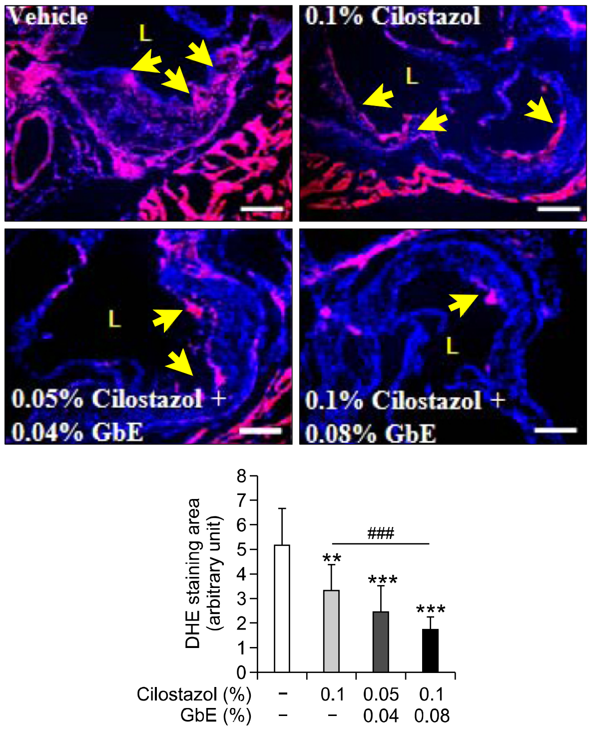

Figure 1. GbE increases the anti-oxidant activity of cilostazol. DHE fluorescence image of aortic root area from vehicle (n = 5), 0.1% cilostazol (n = 9), 0.05% cilostazol + 0.04% GbE (n = 9) and 0.1% cilostazol + 0.08% GbE treated groups (n = 12 each). Quantitative data in the lower graph represent arbitrary units for fluorescence intensity. L, lumen. Yellow arrows indicate superoxide-positive areas. Scale bars, 200 μm. $^{**}P < 0.01$ and $^{***}P < 0.001$ compared with vehicle; and $^{\#\#\#}P < 0.001$ compared with cilostazol alone.

GbE synergistically increases the anti-atherogenic effect of cilostazol

To determine how the anti-oxygenic effect of these two compounds affects the development of atherosclerosis, we analyzed atherosclerotic lesions in ApoE null mice fed a high-fat diet for 16 weeks. Sections of the aortic root from untreated mice showed a large plaque lesion area in the vessel walls. As expected, mice treated with cilostazol (0.1%) and GbE (0.08%) showed a significant reduction in the size of the atherosclerotic lesion in the aortic root (0.48 ± 0.06 mm^2 vs 0.56 ± 0.05 mm^2 in 0.1% cilostazol, 0.08% GbE treatment group and vehicle treatment group, respectively; P = 0.04; Figure 2A). Plaque area in the aortic arch and descending aorta was also reduced in mice treated with cilostazol (0.1%) and GbE (0.08%) compared with control mice (9.26 ± 0.57% vs 11.78 ± 2.5% in 0.1% cilostazol, 0.08% GbE treatment group and vehicle treatment group, respectively; $P = 0.05$; Figure 2B). Total cholesterol and triglyceride levels in serum were significantly decreased in mice treated with 0.1% cilostazol alone, however co-treatment of cilostazol and GbE showed no significant changes (data not shown).

Co-treatment with cilostazol and GbE decreases pro-inflammatory cytokine production

Next, we investigated whether these two compounds can affect the production of pro-inflammatory molecules in blood. The monocyte chemoattractant-1 (MCP-1) level was significantly decreased in mice treated with cilostazol alone and also in those co-treated with a high dose of cilostazol and GbE. The expression level of soluble vascular cell adhesion molecule (sVCAM-1) was significantly decreased in the co-treatment group. However, interleukin-6 (IL-6) levels were not changed in the co-treatment group (Table 1). To confirm the changes of these molecule expressions in the plaque area, we performed immunohistochemistry. Compared with the control group, co-treatment of cilostazol with GbE decreased the expression of MCP-1 (Figure 3A) and VCAM-1 (Figure 3B).

Co-treatment with cilostazol and GbE inhibits macrophage infiltration

We measured infiltrated macrophages in the atherosclerotic plaque area in order to determine if the production of MCP-1 and VCAM-1 lead to a decrease in macrophage infiltration into the aortic intima. Macrophage infiltration was lower in the high dose co-treatment group than cilostazol alone. These data suggest that co-treatment of cilostazol with GbE exerts a synergistic effect on the inhibition of macrophage infiltration into the arterial walls (Figure 4).

Discussion

In this study, we show that co-treatment of cilostazol

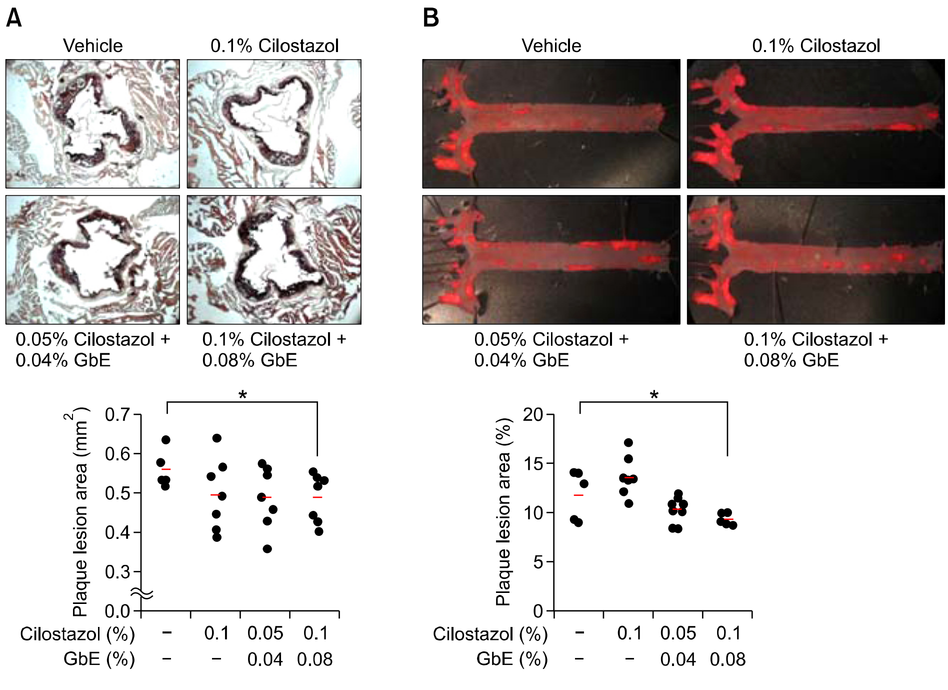

Figure 2. GbE with cilostazol synergistically decreases the atherosclerotic lesion size in aortic root area of ApoE null mice fed a high-fat diet. High dose of cilostazol (0.1%) and GbE (0.08%) treatment reduced fatty streak lesions in ApoE null mice. (A) Oil red O-stained frozen section of aortic sinus from vehicle (n = 5), 0.1% cilostazol (n = 7), 0.05% cilostazol + 0.04% GbE (n = 7) and 0.1% cilostazol + 0.08% GbE (n = 7) treated groups. (B) Aortic en face view of vehicle (n = 5), 0.1% cilostazol (n = 7), 0.05% cilostazol + 0.04% GbE (n = 9) and 0.1% cilostazol + 0.08% GbE (n = 5) treated groups. Representative Oil red O staining of atherosclerotic lesions in each group is shown. Quantitative data in the lower graph represent plaque area. *$P < 0.05$ compared with vehicle.

Table 1. Analysis of serum inflammatory molecules in *ApoE* null mice fed high fat diet supplemented with each compounds

	Vehicle	0.1% cilostazol	0.05% cilostazol + 0.04% GbE	0.1% cilostazol + 0.08% GbE
Mice, n	11	10	12	12
IL-6 (pg/ml)	35.7 ± 17.6	22 ± 5.3	26.6 ± 11.2	29 ± 25.3
MCP-1 (pg/ml)	93.8 ± 28.4	67.9 ± 12.7*	84.1 ± 15.1	70.5 ± 16.8*
sVCAM (ng/ml)	828.5 ± 32.6	825.3 ± 53.3	745.8 ± 23.5**	605.8 ± 11***

Data are expressed as mean ± SEM. *$P < 0.05$, **$P < 0.01$, ***$P < 0.001$ compare to vehicle group. IL-6, interleukin-6; MCP-1, monocyte chemoattractant protein-1; sVCAM-1, soluble vascular cell adhesion molecule-1.

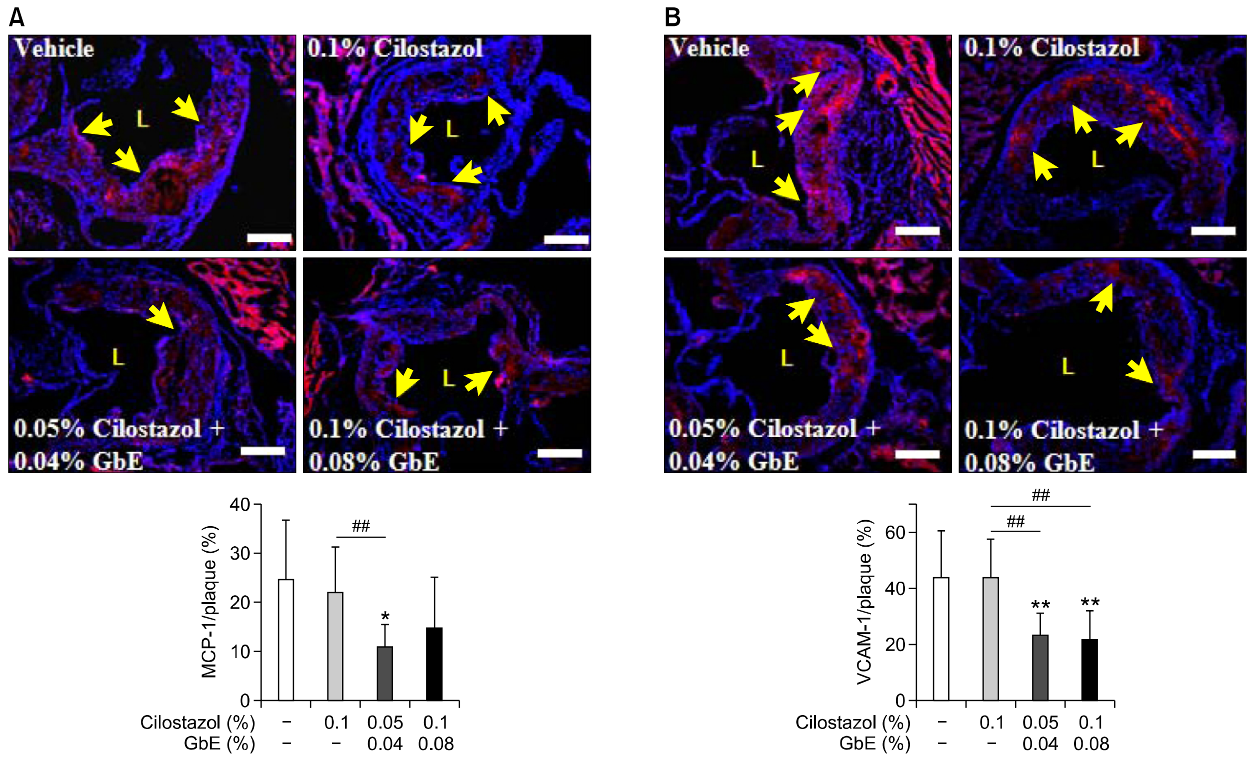

Figure 3. Co-treatment of cilostazol and GbE decreases pro-inflammatory cytokine production. The effect of co-treatment of cilostazol and GbE on MCP-1 (A) and VCAM-1 (B) levels in the atherosclerotic lesion of vehicle (*n* = 7 or 9), 0.1% cilostazol (*n* = 7 or 9), 0.05% cilostazol + 0.04% GbE (*n* = 6 or 9), and 0.1% cilostazol + 0.08% GbE treated groups (*n* = 8 or 10). Representative immunohistochemical staining for MCP-1 and VCAM-1 in each group is also shown. Quantitative data in the lower graph represent positive stained area in the plaque. L, lumen. Yellow arrows indicate MCP-1 and VCAM-1-positive areas. Scale bars, 200 μm. *$P < 0.05$ and **$P < 0.01$ compared with vehicle; $^{\#\#}P < 0.01$ compared with cilostazol alone.

with GbE reduces superoxide production following decreased atherosclerotic plaque formation. Co-treatment of cilostazol with GbE also lowered sVCAM-1 and MCP-1 levels in serum, and reduced macrophage infiltration into the aortic intima. Our observations indicate that cilostazol and GbE exert synergistic anti-atherosclerotic effects. Indeed, we have demonstrated that co-treatment of cilostazol with GbE induced a reduction in atherosclerotic lesion.

Increased ROS generation such as superoxide may be involved in the development of atherosclerosis (Dandona *et al*., 2010). ROS-dependent mechanisms can increase the expression of adhesion molecule such as VCAM-1, leading to inflammatory cell recruitment and infiltration into the intima region (Chen *et al*., 2003; Lee *et al*., 2005; Ou *et al*., 2009). In atherosclerotic conditions, treatment with either cilostazol or GbE markedly attenuates ROS production by a distinct mechanism. Cilostazol blocks ROS production *via* inhibition of NADPH oxidase (Shin *et al*., 2004; Yun *et al*., 2009). It also reduces CD36 or SR-A expression in murine macrophages *via* inhibition of NADPH oxidase-derived ROS production, which leads to reduced foam cell formation (Okutsu *et al*., 2009;

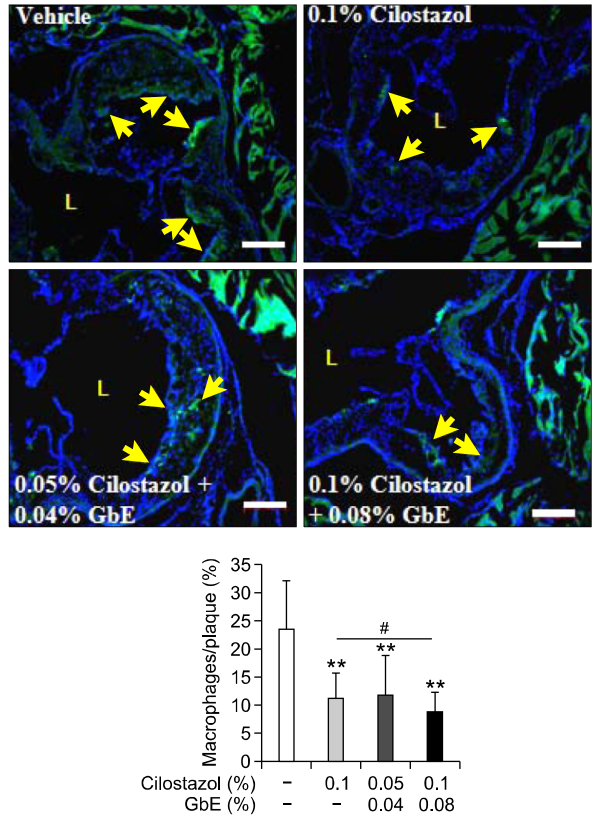

Figure 4. Co-treatment of cilostazol and GbE inhibits macrophage infiltration. Representative immunostaining for macrophages in the aortic root area from vehicle (n = 5), 0.1% cilostazol (n = 10), 0.05% cilostazol + 0.04% GbE (n = 8), and 0.1% cilostazol + 0.08% GbE treated groups (n = 8). Quantitative data in the lower graph represent positive stained area percentage of total plaque area. L, lumen. Yellow arrows indicate a macrophage-positive area. Scale bars, 200 μm. $^{**}P < 0.01$ compared with vehicle; $^{\#}P < 0.05$ compared with cilostazol alone.

Yun *et al*., 2009). A recent study also showed that cilostazol inhibited oxidative stress and subsequent cellular senescence by enhancement of NO production in HUVECs. Cilostazol can induce NO production by eNOS activation *via* a cAMP/PKA- and PI3K/Akt-dependent mechanism, thereby delaying endothelial cellular senescence. Cellular senescence of endothelial cells has been proposed to be involved in endothelial dysfunction and atherosclerosis (Ota *et al*., 2008).

Inflammation is involved in the initiation, rupture, and thrombosis of atherosclerotic plaques (Lee *et al*., 2005). Some studies have suggested that cilostazol and GbE have anti-inflammatory effects (Lippi *et al*., 2007; Mohamed, 2009; Aoki *et al*., 2010). GbE contains high levels of terpene, and this biflavonoid decreases the levels of IL-6, IL-8, and tumor necrosis factor (TNF)-alpha through the down-regulation of NF-κB DNA binding activity in patients with pulmonary interstitial fibrosis (Lippi *et al*., 2007). Previous studies have reported that cAMP selectively suppresses expression of VCAM-1 and endothelial leukocyte adhesion molecule-1 (ELAM-1) (Pober *et al*., 1993). Moreover, VCAM-1 plays a major role in the initiation of atherosclerosis (Cybulsky *et al*., 2001). Given the role of cilotazol as a cAMP activator, these previous findings are in agreement with our results. In addition, MCP-1 is a crucial factor for the development of atherosclerosis. Whereas VCAM-1 exerts a dominant role in the initiation of atherosclerosis, increased MCP-1 expression was demonstrated to mediate chronic inflammation. Both preferentially contribute to monocyte adhesion (Lee *et al*., 2005; Choi *et al*., 2011). We show that elevated macrophage infiltration is accompanied by high expression of VCAM-1 and MCP-1 in serum and the atherosclerotic plaque region. Although MCP-1 levels in serum appear to be mainly affected by cilostazol in our study, the level of MCP-1 in atherosclerotic plaque was decreased by co-treatment with cilostazol and GbE, but not cilostazol alone. These findings all show that atherosclerosis is significantly reduced by co-treatment with cilostazol and GbE compared to treatment with cilostazol alone.

Taken together, the our data support the hypothesis that the anti-atherosclerotic effect of cilostazol and GbE can be attributed to reduced superoxide generation, macrophage infiltration, and expression of pro-inflammatory molecules such as VCAM-1 and MCP-1. The major finding of the present study is that co-treatment of cilostazol with GbE significantly decreased atherosclerotic plaque in the aorta of ApoE null mice fed a high-fat diet, compared to treatment with cilostazol alone. In conclusion, we show that combinative therapy of cilostazol with GbE might exert an enhanced anti-atherogenic effect compared to treatment with cilostazol alone.

Methods

Animals and diets

ApoE null (C57BL/6J background) male mice were purchased from Jackson Laboratories (Bar Harbor, ME) and acclimated to the facility for at least 2 weeks before beginning the experiments. Mice were housed five to six per cage and maintained on a 12-h light/12-h dark cycle with water *ad libitum*. Eight-week-old male ApoE null mice were randomly divided into five groups including: normal chow (n = 5), vehicle (n = 11), cilostazol (n = 10) and both co-treatment groups (n = 12 per group). The animals were fed a high-fat diet (20% fat, 0.15% cholesterol, Research Diets, New Brunswick, NJ) supplemented with 0.1% cilostazol, or both 0.05% cilostazol and 0.04% GbE, or both 0.1% cilostazol and 0.08% GbE for test groups (0.1% lactose for vehicle group) for 16 weeks respectively. Control mice were fed ordinary normal chow diet (PMI® Nutrition International, LLC Certified Rodent LABDIET® 5002, Purina Mills, Richmond, IN). Body weights were monitored every week. All animal study protocols were approved by the Institutional Animal Care and Usage Committee of the Ewha Womans University (Seoul, Korea).

Genotyping

Genotyping was performed to confirm ApoE deficiency. Genomic DNA was extracted from mouse tails. For PCR of ApoE, the forward and reverse primers for the wild type allele were 5'-AGAACTGACGTGAGTGTCCA-3' and 5'-GTT CCCAGAAGTTGAGAAGC-3' (expected product -300 bp), respectively. For the null allele, the same forward primer was used and the reverse primer was 5'-GCTTCCTCGTG CTTTACGGTA-3' (expected product -200 bp). PCR was carried out with all three primers in the same reaction mix. PCR conditions were: 94°C, 45 s; 58°C, 45 s; and 72°C, 45 s for 30 cycles.

Atherosclerosis quantification

After mice were euthanized, hearts and aortas were perfused with phosphate-buffered saline (PBS) through the left ventricle. The aortas were dissected from the proximal ascending aorta to the bifurcation of the iliac artery, and adventitial fat was removed. After aortas were opened longitudinally, these were pinned onto a flat black silicone plate with 2 cm needles. The hearts and pinned aortas were fixed with 10% neutral buffered formalin solution for 16 h. For lesion quantification in the aortic root, the hearts were removed at the proximal aorta and the upper portion was embedded in OCT compound (Tissue-Tek) and frozen at -70°C. Ventricular tissue was sectioned into 10 μm sections by a cryostat microtome (Leica CM18050 XL). Sections and fixed aortas were immersed in absolute propylene glycol (Duchefa Biochemie) for 1 min and stained with oil red O (Sigma Aldrich) for 16 h. The samples were immersed in 85% propylene glycol for 2 min, washed with PBS, and then digitally photographed at a fixed magnification. The area occupied by the lesion in the aortic root was measured using Axiovision AC (Carl Zeiss, Germany). To quantify *en face* lesions, the lesion area was evaluated as a percentage of total aortic area.

Blood and cytokine analysis

Blood was collected from the retro-orbital sinus into non-heparinized capillary tubes (Scientific Glass, Inc). Thereafter serum was obtained by centrifugation at 13,000 *g* for 10 min at 4°C and stored at -70°C before analysis. Total cholesterol, triglyceride, HDL, and LDL cholesterol levels were measured. To quantify cytokines in serum, MCP-1 and sVCAM-1 levels were estimated using ELISA kits (R&D Systems).

Measurement of superoxide *in situ.*

The frozen sections of aortic root in the slide were dried for 2 h at 37°C and washed with distilled water for 5 min. The samples were incubated to expose antigen with PBS + 0.1% Triton X-100 (Juncei Chemical Co., Ltd.) for 15 min and then incubated with 5 μM dihydroethidium (Molecular Probes, Eugene, OR) in a light-shielded state to estimate superoxide levels. The washing step was performed with PBS + 0.1% Triton X-100 buffer at least three times for 5 min per wash. After treatment of DAPI solution (Sigma Aldrich) for 30 min, images were observed using a fluorescence microscope (Axiovert 200 Basic Stand, Carl Zeiss, Inc.). The quantitative analysis is expressed as a percentage of DHE-stained area per total lesion area in the aortic root using Axiovision AC (Carl Zeiss, Inc.).

Immunohistochemistry

Cryosection slides were used in immunohistochemical studies. The aortic root was fixed in 10% neutral buffered formalin and then cut into 10-μm-thick sections. Briefly, after dehydration, antigen retrieval was carried out with PBS + 0.1% Triton X-100 for 15 min at room temperature (RT) and the blocking step was performed with Ultra V block (Thermoscientific) for 5 min at RT. Fixed tissue was incubated with primary antibodies against MOMA-2 (Serotec), VCAM-1 (R&D Systems), and MCP-1 (Santa Cruz Biotechnology) for 16 h at 4°C. Except the fluorescein labeled primary antibody, chicken anti-goat, anti-rabbit Alexa 488, 594 (Invitrogen) antibodies were used as a second step to visualize the antigen. After mounting, images were observed using a fluorescence microscope (Axiovert 200 Basic Stand, Carl Zeiss, Inc.). Quantitative analysis of the stained area in the aortic root was measured using Axiovision AC (Carl Zeiss Inc.).

Statistical analysis

Statistical significance was determined by the Student's *t*-test and Mann-Whitney *U* Test. A value of $P < 0.05$ was considered significant.

Acknowledgements

We thank SK chemicals for supporting this study. This study was supported by a grant from the Korea Health 21 R&D Project, Ministry of Health & Welfare (A090264), Korea.

References

Altiok N, Ersoz M, Karpuz V, Koyuturk M. Ginkgo biloba extract regulates differentially the cell death induced by hydrogen peroxide and simvastatin. Neurotoxicology 2006;27:158-63

Aoki C, Hattori Y, Tomizawa A, Jojima T, Kasai K. Anti-inflammatory role of cilostazol in vascular smooth muscle cells *in vitro* and *in vivo*. J Atheroscler Thromb 2010;17:503-9

Chen JW, Chen YH, Lin FY, Chen YL, Lin SJ. Ginkgo biloba extract inhibits tumor necrosis factor-alpha-induced reactive oxygen species generation, transcription factor activation, and cell adhesion molecule expression in human aortic endothelial cells. Arterioscler Thromb Vasc Biol 2003;23: 1559-66

Choi JH, Park JG, Jeon HJ, Kim MS, Lee MR, Lee MN, Sonn SK, Kim JH, Lee MH, Choi MS, Park YB, Kwon OS, Jeong TS, Lee WS, Shim HB, Shin DH, Oh GT. 5-(4-Hydroxy-2,3,5-trimethylbenzylidene) thiazolidine-2,4-dione attenuates atherosclerosis possibly by reducing monocyte recruitment to the lesion. Exp Mol Med 2011;43:471-8

Cybulsky MI, Iiyama K, Li H, Zhu S, Chen M, Iiyama M, Davis V, Gutierrez-Ramos JC, Connelly PW, Milstone DS. A major role for VCAM-1, but not ICAM-1, in early atherosclerosis. J Clin Invest 2001;107:1255-62

Dandona P, Ghanim H, Chaudhuri A, Dhindsa S, Kim SS. Macronutrient intake induces oxidative and inflammatory stress: potential relevance to atherosclerosis and insulin resistance. Exp Mol Med 2010;42:245-53

Gomez CR, Qureshi AI. Medical treatment of patients with intracranial atherosclerotic disease. J Neuroimaging 2009; 19:25S-9S

Hattori Y, Suzuki K, Tomizawa A, Hirama N, Okayasu T, Hattori S, Satoh H, Akimoto K, Kasai K. Cilostazol inhibits cytokine-induced nuclear factor-kappaB activation *via* AMP-activated protein kinase activation in vascular endothelial cells. Cardiovasc Res 2009;81:133-9

Kampkotter A, Pielarski T, Rohrig R, Timpel C, Chovolou Y, Watjen W, Kahl R. The Ginkgo biloba extract EGb761 reduces stress sensitivity, ROS accumulation and expression of catalase and glutathione S-transferase 4 in Caenorhabditis elegans. Pharmacol Res 2007;55:139-47

Kim KY, Shin HK, Choi JM, Hong KW. Inhibition of lipopolysaccharide-induced apoptosis by cilostazol in human umbilical vein endothelial cells. J Pharmacol Exp Ther 2002;300:709-15

Kim MJ, Lee JH, Park SY, Hong KW, Kim CD, Kim KY, Lee WS. Protection from apoptotic cell death by cilostazol, phosphodiesterase type III inhibitor, *via* cAMP-dependent protein kinase activation. Pharmacol Res 2006;54:261-7

Lee JH, Oh GT, Park SY, Choi JH, Park JG, Kim CD, Lee WS, Rhim BY, Shin YW, Hong KW. Cilostazol reduces atherosclerosis by inhibition of superoxide and tumor necrosis factor-alpha formation in low-density lipoprotein receptor-null mice fed high cholesterol. J Pharmacol Exp Ther 2005;313: 502-9

Lee TM, Su SF, Hwang JJ, Tseng CD, Chen MF, Lee YT, Wang SS. Differential lipogenic effects of cilostazol and pentoxifylline in patients with intermittent claudication: potential role for interleukin-6. Atherosclerosis 2001;158: 471-6

Lim JH, Woo JS, Shin YW. Cilostazol protects endothelial cells against lipopolysaccharide-induced apoptosis through ERK1/2- and P38 MAPK-dependent pathways. Korean J Intern Med 2009;24:113-22

Lippi G, Targher G, Guidi GC. Ginkgo biloba, inflammation and lipoprotein(a). Atherosclerosis 2007;195:417-8

Liu HJ, Wang XL, Zhang L, Qiu Y, Li TJ, Li R, Wu MC, Wei LX, Rui YC. Inhibitions of vascular endothelial growth factor expression and foam cell formation by EGb 761, a special extract of Ginkgo biloba, in oxidatively modified low-density lipoprotein-induced human THP-1 monocytes cells. Phytomedicine 2009;16:138-45

Mohamed RH. Role of cilostazol in alleviating cardiovascular complications induced in experimental rats through regulation of type 1 plasminogen activator inhibitor and transforming growth factor-beta(1) overexpression. Biomed Pharmacother 2009;12:12

Nakamura N, Osawa H, Yamabe H, Okumura K, Hamazaki T. Effects of cilostazol on lipid and fatty acid metabolism. Clin Exp Med 2005;4:170-3

Nakaya K, Ayaori M, Uto-Kondo H, Hisada T, Ogura M, Yakushiji E, Takiguchi S, Terao Y, Ozasa H, Sasaki M, Komatsu T, Ohsuzu F, Ikewaki K. Cilostazol enhances macrophage reverse cholesterol transport *in vitro* and *in vivo*. Atherosclerosis 2010;213:135-41

Okutsu R, Yoshikawa T, Nagasawa M, Hirose Y, Takase H, Mitani K, Okada K, Miyakoda G, Yabuuchi Y. Cilostazol inhibits modified low-density lipoprotein uptake and foam cell formation in mouse peritoneal macrophages. Atherosclerosis 2009;204:405-11

Ota H, Eto M, Kano MR, Ogawa S, Iijima K, Akishita M, Ouchi Y. Cilostazol inhibits oxidative stress-induced premature senescence *via* upregulation of Sirt1 in human endothelial cells. Arterioscler Thromb Vasc Biol 2008;28:1634-9

Otsuki M, Saito H, Xu X, Sumitani S, Kouhara H, Kurabayashi M, Kasayama S. Cilostazol represses vascular cell adhesion molecule-1 gene transcription *via* inhibiting NF-kappaB binding to its recognition sequence. Atherosclerosis 2001; 158:121-8

Ou HC, Lee WJ, Lee IT, Chiu TH, Tsai KL, Lin CY, Sheu WH. Ginkgo biloba extract attenuates oxLDL-induced oxidative functional damages in endothelial cells. J Appl Physiol 2009;106:1674-85

Park SY, Lee JH, Shin HK, Kim CD, Lee WS, Rhim BY, Shin YW, Hong KW. Synergistic efficacy of concurrent treatment with cilostazol and probucol on the suppression of reactive oxygen species and inflammatory markers in cultured human coronary artery endothelial cells. Korean J Physiol Pharmacol 2008;12:165-70

Pober JS, Slowik MR, De Luca LG, Ritchie AJ. Elevated cyclic AMP inhibits endothelial cell synthesis and expression of TNF-induced endothelial leukocyte adhesion molecule-1, and vascular cell adhesion molecule-1, but not intercellular adhesion molecule-1. J Immunol 1993;150:5114-23

Rhein V, Giese M, Baysang G, Meier F, Rao S, Schulz KL, Hamburger M, Eckert A. Ginkgo biloba extract ameliorates oxidative phosphorylation performance and rescues abeta-induced failure. PLoS One 2010;5:e12359

Rodriguez M, Ringstad L, Schafer P, Just S, Hofer HW, Malmsten M, Siegel G. Reduction of atherosclerotic nanoplaque formation and size by Ginkgo biloba (EGb 761) in cardiovascular high-risk patients. Atherosclerosis 2007; 192:438-44

Ryu KH, Han HY, Lee SY, Jeon SD, Im GJ, Lee BY, Kim K, Lim KM, Chung JH. Ginkgo biloba extract enhances antiplatelet and antithrombotic effects of cilostazol without prolongation of bleeding time. Thromb Res 2009;124: 328-34

Sethi A, Arora RR. Medical management and cardiovascular risk reduction in peripheral arterial disease. Exp Clin Cardiol 2008;13:113-9

Shin HK, Kim YK, Kim KY, Lee JH, Hong KW. Remnant lipoprotein particles induce apoptosis in endothelial cells by NAD(P)H oxidase-mediated production of superoxide and cytokines *via* lectin-like oxidized low-density lipoprotein receptor-1 activation: prevention by cilostazol. Circulation 2004;109:1022-8

Siegel G, Schafer P, Winkler K, Malmsten M. Ginkgo biloba (EGb 761) in arteriosclerosis prophylaxis. Wien Med Wochenschr 2007;157:288-94

Wang T, Elam MB, Forbes WP, Zhong J, Nakajima K. Reduction of remnant lipoprotein cholesterol concentrations by cilostazol in patients with intermittent claudication. Atherosclerosis 2003;171:337-42

Wei Z, Peng Q, Lau BH, Shah V. Ginkgo biloba inhibits hydrogen peroxide-induced activation of nuclear factor kappa B in vascular endothelial cells. Gen Pharmacol 1999;33:369-75

Yun MR, Park HM, Seo KW, Kim CE, Yoon JW, Kim CD. Cilostazol Attenuates 4-hydroxynonenal-enhanced CD36 Expression on Murine Macrophages *via* Inhibition of NADPH Oxidase-derived Reactive Oxygen Species Production. Korean J Physiol Pharmacol 2009;13:99-106

Zhou LJ, Zhu XZ. Reactive oxygen species-induced apoptosis in PC12 cells and protective effect of bilobalide. J Pharmacol Exp Ther 2000;293:982-8